Journal of Sound and Vibration 329 (2010) 5397–5414

Contents lists available at ScienceDirect

Journal of Sound and Vibration

journal homepage: www.elsevier.com/locate/jsvi

Optimal active absorber with internal state feedback for controlling resonant and transient vibration

S. Chatterjee*

Department of Mechanical Engineering, Bengal Engineering and Science University, Shibpur, Howrah 711 103, West Bengal, India

ARTICLE INFO

Article history:
Received 6 November 2009
Received in revised form
16 July 2010
Accepted 16 July 2010
Handling Editor: J. Lam
Available online 9 August 2010

ABSTRACT

An active, standalone vibration absorber utilizing the state feedback taken from the absorber mass is proposed. Expressions of the optimum absorber parameters are obtained both by optimizing the H_∞ norm of the frequency response function. For improved transient response featuring low peak response and fast attenuation, the design procedure utilizes the mode equalization followed by the maximization of the damping. An interesting feature of the proposed absorber is that the performance of the absorber does not require having its natural frequency close to the natural frequency of the primary system as is generally the case for tuned passive absorbers or other active and semi-active tuned vibration absorbers. In fact, the performance of the proposed system can be progressively enhanced by increasing the absorber frequency. Compared to the optimum passive absorber, the optimal active absorber can yield wider bandwidth of operation around the natural frequency of the primary system and lower frequency response within the suppression band. The active absorber also offers better transient response compared to the passive absorber both optimized for the best transient responses. The efficacy of the absorber is analyzed both for a single-degree-of-freedom and beam like primary structure.

1. Introduction

Tuned vibration absorbers (TVA) have been used and studied innumerable times in different ways since Frahm [1] patented it. When tuned to the frequency of forced vibration of a structure, the device can completely eliminate the vibration by creating an anti-resonance at the frequency of vibration. However, any change in the frequency of vibration from the tuned frequency renders the device largely ineffective. Additional damping [2] in the absorber can limit the maximum response of the primary system at resonances sacrificing the performance at the tuned frequency. The major drawback of the passive TVA is that it is suitable only for a narrow bandwidth of operation and therefore, it is useful in eliminating single frequency resonant vibrations. However, multiple TVAs can suppress vibrations with number of tonal frequencies [3].

Past few decades have witnessed a large number of research works aiming to overcome the aforesaid shortcoming of the passive TVA by increasing the suppression bandwidth of the TVA. A major proportion of these studies consider the application of active TVAs. Active TVAs utilize an actuator in parallel with the spring and the damper of the passive TVA. This adds flexibility to incorporate control theory to provide cancellation forces. In order to reduce the energy expenditure of the active devices, several semi-active versions of the TVAs are also proposed. Semi-active TVAs can alter the system parameters using minimal energy. Systems can have variable inertia, variable damping, variable stiffness, or variable initial

* Tel.: +91 9836596135.
E-mail addresses: shychat@gmail.com, shy@mech.becs.ac.in

0022-460X/$ - see front matter © 2010 Elsevier Ltd. All rights reserved.
doi:10.1016/j.jsv.2010.07.017

conditions. Adaptive tuned vibration absorbers use an algorithm that tunes the absorber as conditions change. Since the adaptive TVA is capable of changing its resonance frequency, it has an increased effective bandwidth over classical devices. The majority of works in this area focus on the control law issues. The active vibration absorber is still a very relevant field of research. Exhaustive reviews of the literature on the subject are available in Refs. [4–6].

A majority of the earlier studies focus on the suitable control law for the active vibration absorber that widens the operating bandwidth. Most of these control laws are based on the displacement, velocity and/or acceleration feedback taken from the primary structure. The present paper studies the efficacy of an active absorber that runs on its internal feedback, i.e., the feedback is taken from the absorber mass itself. This standalone feature of the absorber has an attractive commercial value because of its user friendliness, because the user has to simply attach the device to the vibrating body. Only a very few studies on such class of devices are available as reported below.

Olgac and co-workers [7–10] develop the *delayed resonator* (DR) concept to provide active control of a TVA. The *delayed resonator absorber* (DRA) provides an interesting approach; it uses time-delayed position, velocity or acceleration feedback of the absorber mass. As a result, the active absorber turns into a standalone device that runs on its internal feedback without requiring any feedback from the primary structure. The device operates on the principle of converting the absorber into a perfect resonator by placing a pair of dominant poles on the imaginary axis. An adaptive tuning algorithm decides the location of the pair of poles, and hence the natural frequency of the absorber. The vibration absorption is achieved when the natural frequency of the absorber is tuned to the operating frequency. Knowles et al. [11] introduce the concept of *active resonator absorber* (ARA) very akin to the concept of the DR absorber. In ARA, the absorber can be converted into a perfect resonator by utilizing any type of feedback. Elmali et al. [12] study the efficacy of the ARA using the state (position and velocity) feedback of the absorber mass. They also show that ARA has theoretically infinite frequency range of tunability whereas the DR has only limited frequency range of tunability.

When adaptively used, a DR absorber or ARA can tune only to a single excitation frequency and perfectly (theoretically zero amplitude of vibration) control the vibration at that frequency. However, just below and above the control frequency, the DR (or ARA), like the passive absorber, introduces two resonant frequencies. As a result, the combined system becomes vulnerable to any excitation containing spectral components at these two frequencies. Widening the operating bandwidth around resonant frequency of the primary structure can overcome this problem. This is achieved by using the device in the optimal active absorber mode without the auto-tuning feature. Under these circumstances, the optimum absorber is tuned to the resonant frequency of the primary structure and the poles of the combined system are placed in the desired location by optimally selecting the control parameters. The device is particularly suitable for controlling wide-band vibrations around the resonant frequency of the primary structure. Jalili and Olgac [13,14] study the performance of the optimal absorber utilizing the time-delayed acceleration feedback of the absorber mass. They show that the optimal active absorber performs better than an optimal passive absorber.

Okada et al. [15] study the effectiveness of an active absorber with voice coil actuator. They present a novel circuit to provide sensing and actuation in a voice coil design. The velocity is estimated based on the driving voltage and current. This self-sensing active TVA is experimentally demonstrated. Rivaz and Rohling [16] report the efficacy of an active absorber (PI-DVA) for hand-held devices. The absorber is controlled by the acceleration feedback taken from the absorber mass. Their study concentrates on the transient response of the combined system. Comparisons with the other types of the control, like PD (proportional derivative) and DR reveal that the PI-DVA can be slightly more efficient in controlling the vibration of hand-held devices.

The present paper analyses the dynamic characteristics of an optimal standalone active vibration absorber running on the internal state feedback (PD control) taken from the absorber mass. Fundamentally, the absorber comprises of a spring–mass system attached to a rigid base and an actuator placed parallel to the spring in between the base and the mass. The actuator is controlled by the state feedback taken from the oscillating mass of the absorber itself. The optimal frequency and transient response characteristics of the absorber are first analyzed considering a single-degree-of-freedom primary system. The performance of the optimal active absorber is compared with that of an optimal passive vibration absorber. The analysis is further extended to an elastic Euler–Bernoulli beam.

2. Single-degree-of-freedom primary system

2.1. Mathematical model

A model of the single-degree-of-freedom primary system with the active absorber attached to it is illustrated in Fig. 1. The primary structure is a single-degree-of-freedom undamped oscillator having the primary mass M suspended by a spring of stiffness K. The absorber consists of a secondary mass m attached to the primary structure by a spring of stiffness K_a. An actuator placed in between the primary and the secondary mass exerts the control force F_c. X and Y are the absolute displacements of the primary and the secondary mass, respectively. Equations of motion of the combined two-degrees-of-freedom system illustrated in Fig. 1 read as

$$MX'' + KX + K_a(X - Y) = F(t^*) - F_c, \tag{1}$$

$$mY'' + K_a(Y - X) = F_c, \tag{2}$$

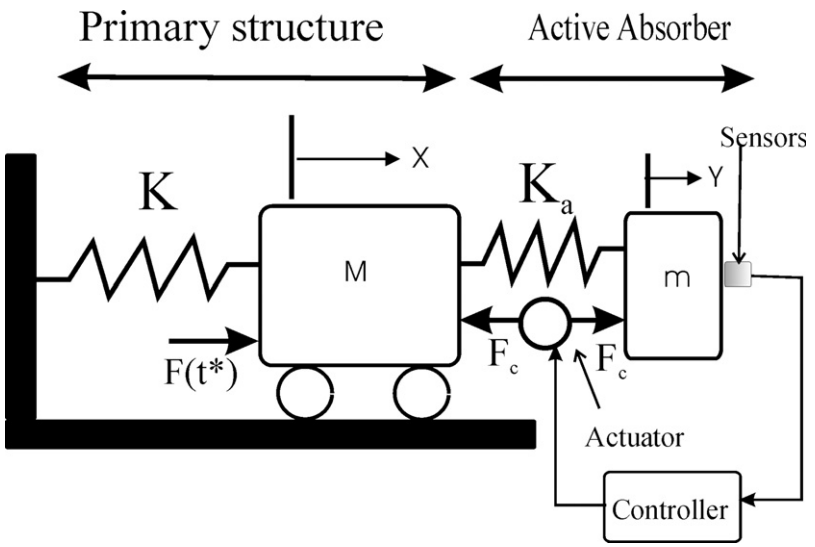

Fig. 1. Model of the single-degree-of-freedom oscillator with the active absorber.

where $F(t^*)$ is the dynamic load acting on the primary system and the 'dash' denotes the derivative with respect to time t^* in Eqs. (1) and (2).

In order to simplify the analysis, the actuator is considered to be an ideal force generator. This is indeed a valid assumption within a specific range of the operating frequency depending upon the actuator. For example, an electromagnetic actuator may be treated as an ideal force generator within the bandwidth of its LR circuit [17]. Thus, neglecting the actuator dynamics the control force (F_c) is expressed as

$$F_c = K_p Y - K_v Y', \tag{3}$$

where K_p and K_v are the control gains.

Eqs. (1) and (2) can be recast in the following non-dimensional form:

$$\begin{bmatrix} 1 & 0 \\ 0 & \mu \end{bmatrix} \begin{Bmatrix} \ddot{x} \\ \ddot{y} \end{Bmatrix} + \begin{bmatrix} 1+\mu\omega_a^2 & -\mu\omega_a^2 \\ -\mu\omega_a^2 & \mu\omega_a^2 \end{bmatrix} \begin{Bmatrix} x \\ y \end{Bmatrix} = \begin{Bmatrix} f(t) \\ 0 \end{Bmatrix} + \begin{Bmatrix} -f_c \\ f_c \end{Bmatrix}, \tag{4}$$

with the following non-dimensional quantities:

$$\text{Non-dimensional deflection of the primary mass} : x = \frac{X}{x_0},$$

$$\text{non-dimensional deflection of the secondary mass} : y = \frac{Y}{x_0},$$

$$\text{mass ratio} : \mu = \frac{m}{M},$$

$$\text{non-dimensional absorber frequency} : \omega_a = \frac{\omega_a^*}{\omega_0},$$

where x_0 is an arbitrary length (may be the static deflection of the primary oscillator), $\omega_0 = \sqrt{K/M}$ is the natural frequency of the primary system and $\omega_a^* = \sqrt{K_a/m}$ is the natural frequency of the absorber.

The 'dot' denotes differentiation with respect to the non-dimensional time $t = \omega_0 t^*$.

The non-dimensional control force is obtained from Eq. (3) and given as

$$f_c = k_p y - k_v \dot{y}, \tag{5}$$

where the non-dimensional control gains are $k_p = K_p/M\omega_0^2$ and $k_v = K_v/M\omega_0$.

2.2. Frequency response analysis

Taking the Laplace Transformation of Eqs. (4) and (5), yields the transfer function relating the displacement of the primary system and the excitation force as

$$G(s) = \frac{X(s)}{F(s)} = \frac{s^2 + (k_v/\mu)s + \omega_a^2 - (k_p/\mu)}{s^4 + a_3 s^3 + a_2 s^2 + a_1 s + a_0}. \tag{6}$$

And the transfer function relating the absorber deflection and the excitation force is obtained as

$$G_a(s) = \frac{X(s) - Y(s)}{F(s)} = \frac{s^2 + (k_v/\mu s) - (k_p/\mu)}{s^4 + a_3 s^3 + a_2 s^2 + a_1 s + a_0}, \tag{7}$$

where $a_3 = a_1 = k_v/\mu$, $a_2 = 1 + \mu\omega_a^2 + \omega_a^2 - k_p/\mu$, and $a_0 = \omega_a^2 - k_p/\mu$.

The stability of the static equilibrium of the combined system can be analyzed by applying the Routh–Hurwitz criterion to the characteristic equation of the system given by

$$s^4 + a_3 s^3 + a_2 s^2 + a_1 s + a_0 = 0. \tag{8}$$

The combined system is stable if the following conditions are satisfied:

$$a_1 = a_3 > 0, \quad a_2 > a_0 + 1 \quad \text{and} \quad a_0 > 0. \tag{9}$$

As the mass ratio $\mu > 0$, the conditions given in Eq. (9) finally culminate into the following two conditions:

$$k_v > 0 \quad \text{and} \quad k_p < \mu\omega_a^2. \tag{10}$$

2.2.1. Optimization of the control parameters: H_∞ optimization

One of the major objectives of the present study is to find the optimal parameters of the absorber. Several optimization criteria have been discussed in the literature, viz., H_∞ and H_2 optimization, etc. [18]. In H_∞ optimization, the objective is to minimize the maximum value of the *frequency response function* (FRF) (called the H_∞ norm) of the primary system. In the present section, H_∞ optimization criterion is used for obtaining the expressions of the optimal control parameters (k_p and k_v) of the absorber. The formal fixed-point theory [19] is employed for the purpose.

The influence of the control parameters on the frequency response characteristics can be understood from Fig. 2. It is observed from Fig. 2 that for a selected value of k_p, the displacement frequency response curves of the primary mass with the absorber always intersect the frequency response curve without the absorber at the two fixed points the locations of which are independent of the value of k_v. The analytical proof of the existence of these two fixed points irrespective of the value of k_v is given in Appendix A. The frequencies (ω_1 and ω_2) corresponding to these two fixed points mark the upper and the lower threshold of the suppression band, where the FRF values of the system with the absorber stays below that without the absorber. The location as well as the width of the suppression band is controlled solely by the gain parameter k_p. One finds these two frequencies ω_1 and ω_2 by solving the following equation:

$$\omega^4 - \frac{1}{2}(a_2 + a_0 + 1)\omega^2 + a_0 = 0. \tag{11}$$

As ω_1 and ω_2 are the two roots of Eq. (11), one can write

$$\omega_1^2 + \omega_2^2 = \frac{1}{2}(a_2 + a_0 + 1) = 1 + \omega_a^2 + \frac{1}{2}\mu\omega_a^2 - \frac{k_p}{\mu}. \tag{12}$$

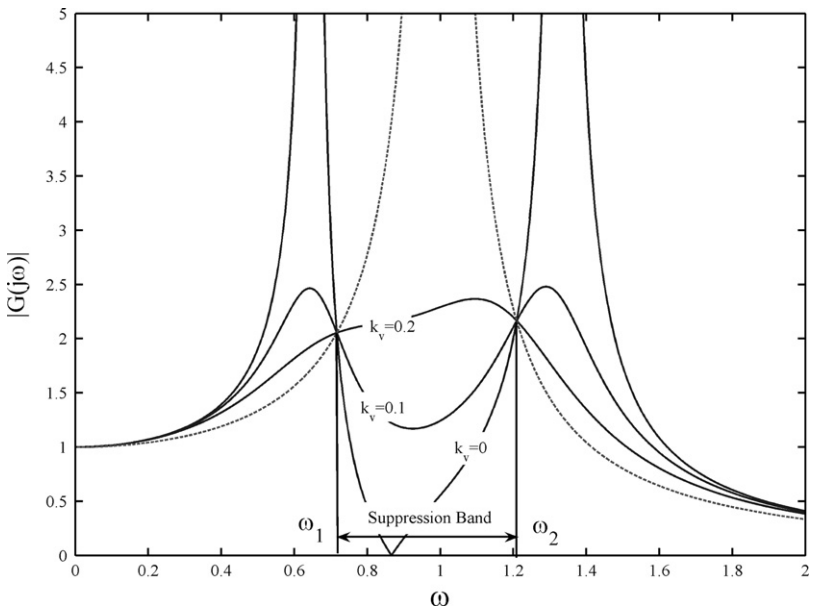

Fig. 2. Typical frequency response plots of the system with and without absorber: - - - - - , without absorber; _____, with absorber, k_p=0.3, ω_a=1.5, μ=0.2.

Clearly the optimum value of the parameter k_p should yield equal FRF values [19] at these two frequencies, when one writes (as the FRF is independent of k_v at these frequencies, consider k_v=0)

$$\frac{1}{\omega_2^2-1}=\frac{1}{1-\omega_1^2}. \tag{13}$$

Eq. (13) simplifies to

$$\omega_1^2+\omega_2^2=2. \tag{14}$$

Substituting (12) in Eq. (14), yields the optimum value of k_p as

$$(k_p)_{opt}=\mu\left[\omega_a^2\left(\frac{\mu}{2}+1\right)-1\right]. \tag{15}$$

For the optimum value of k_p given above, the two frequencies ω_1 and ω_2 are obtained after solving Eq. (11) as

$$\omega_{1,2}^2=1\pm\omega_a\sqrt{\frac{\mu}{2}}. \tag{16}$$

After obtaining the optimal value of the parameter k_p, the other gain parameter k_v should be appropriately adjusted to shape the FRF optimally such that the two peaks of the frequency response plot become equal and occur at the two fixed points. Thus, one writes the optimality conditions as

$$|G(\mathrm{j}\omega_1)|=|G(\mathrm{j}\omega_2)|, \tag{17}$$

$$\frac{\partial}{\partial\omega}|G(\mathrm{j}\omega)|_{\omega=\omega_1}=0, \tag{18}$$

$$\frac{\partial}{\partial\omega}|G(\mathrm{j}\omega)|_{\omega=\omega_2}=0. \tag{19}$$

Clearly Eq. (17) is automatically satisfied by the optimal selection of the parameter k_p. However, Eqs. (18) and (19) cannot be satisfied simultaneously. Under this situation, one can obtain the two quasi-optimal solutions of k_v as the positive solutions of Eqs. (18) and (19), respectively. Rewriting Eq. (18), yields

$$g_4k_v^4+g_2k_v^2+g_0=0, \tag{20}$$

where

$$g_4=\frac{\omega_a(2\sqrt{2}+\sqrt{2}\mu\omega_a^2-4\omega_a\sqrt{\mu})}{2\mu^{7/2}},\quad g_2=-\frac{1}{2}\mu\omega_a^6+\sqrt{\frac{\mu}{2}}\omega_a^5+\omega_a^4-\sqrt{\frac{2}{\mu}}\omega_a^3\quad\text{and}$$

$$g_0=\frac{\omega_a^5}{16}\left(\sqrt{2}\mu^{9/2}\omega_a^4-12\sqrt{2}\mu^{7/2}\omega_a^2+32\mu^3\omega_a-12\sqrt{2}\mu^{5/2}\right)$$

The positive solution of Eq. (20) gives one quasi-optimal value of k_v=$(k_v)_1$ as

$$(k_v)_1^2=\frac{\mu^{5/2}\omega_a^2\left[\mu^2\omega_a^3+2\sqrt{2\mu}-2\mu\omega_a-\sqrt{2}\mu^{3/2}\omega_a^2+2\sqrt{2}\sqrt{\left\{\mu\left(12\mu\omega_a^2-4\sqrt{2}\mu^{3/2}\omega_a^3-8\omega_a\sqrt{2\mu}+\mu^2\omega_a^4+4\right)\right\}}\right]}{2\sqrt{2}\mu\omega_a^2-8\sqrt{\mu}\omega_a+4\sqrt{2}}. \tag{21}$$

Similarly rewriting Eq. (19), yields

$$h_4k_v^4+h_2k_v^2+h_0=0, \tag{22}$$

where $h_4=-\omega_a^2/\mu^3-\omega_a^3/\sqrt{2}\mu^{5/2}-\sqrt{2}\omega_a/\mu^{7/2}$, $h_2=-1/2\mu\omega_a^6-\sqrt{\mu/2}\omega_a^5+\omega_a^4+\sqrt{2/\mu}\omega_a^3$ and $h_0=-\sqrt{2}/16\omega_a^9\mu^{9/2}+3\sqrt{2}/4\omega_a^7\mu^{7/2}+2\omega_a^6\mu^3+3\sqrt{2}/4\omega_a^5\mu^{5/2}$.

The positive solution of Eq. (22) gives the other quasi-optimal value of k_v=$(k_v)_2$ as

$$(k_v)_2^2=\frac{\mu^{5/2}\omega_a^2\left[-\mu^2\omega_a^3+2\sqrt{2\mu}+2\mu\omega_a-\sqrt{2}\mu^{3/2}\omega_a^2+2\sqrt{2}\sqrt{\left\{\mu\left(12\mu\omega_a^2+4\sqrt{2}\mu^{3/2}\omega_a^3+8\omega_a\sqrt{2\mu}+\mu^2\omega_a^4+4\right)\right\}}\right]}{2\sqrt{2}\mu\omega_a^2+8\sqrt{\mu}\omega_a+4\sqrt{2}}. \tag{23}$$

Finally, the average of the two values of k_v as computed from Eqs. (21) and (23) is accepted as the optimal solution of k_v given in Eq. (24)

$$(k_v)_{\mathrm{opt}}=\frac{1}{2}\{(k_v)_1+(k_v)_2\}. \tag{24}$$

Fig. 3 shows the typical displacement frequency response plots of the primary system with the active absorber for the optimum values of the control gains. Using Eqs. (15) and (24) in Eq. (6), one finds the following approximate expression of

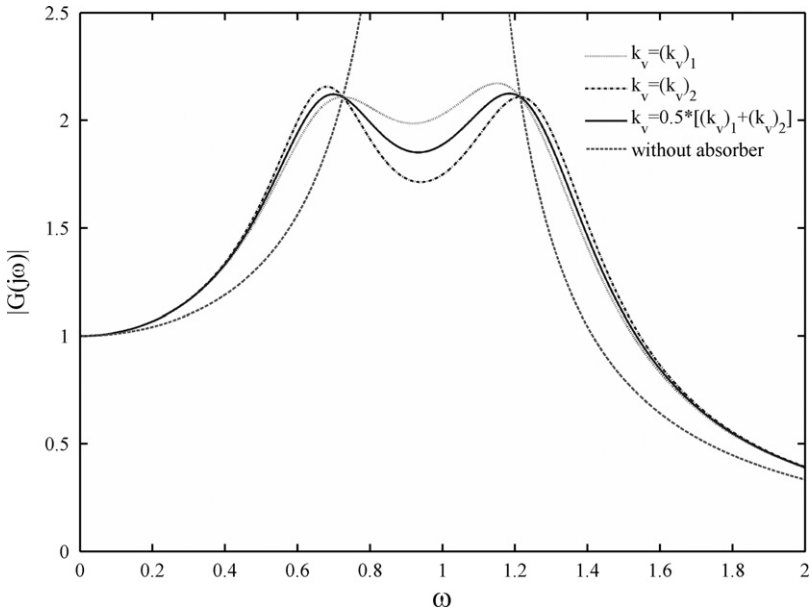

Fig. 3. Optimal displacement frequency response plots of the primary mass: ω_a=1.5, μ=0.2.

the peak value of the displacement FRF of the primary mass of the system with the optimal absorber:

$$|G(j\omega)|_{\max} \approx \frac{\sqrt{2}}{\omega_a\sqrt{\mu}}. \tag{25}$$

From Eqs. (16) and (25) one can infer that for a chosen value of the mass ratio (as permitted by practical circumstances), the width of the suppression band increases and the peak value of the frequency response decreases with the increasing value of the absorber frequency. An interesting feature of the proposed absorber is that the performance of the absorber does not require having its natural frequency close to the natural frequency of the primary system as is generally required in case of the tuned passive absorber or other active and semi-active tuned vibration absorbers. The higher is the absorber frequency the better is its performance. However, the maximum value of the absorber frequency is limited by the stability requirement as spelt out in Eq. (10). Using Eq. (15) in Eq. (10), one can show that the upper threshold value of ω_a is limited by

$$\omega_a < \sqrt{\frac{2}{\mu}}. \tag{26}$$

Eqs. (25) and (26) clearly suggest that under no circumstances, the peak value of the frequency response can be less than unity.

Fig. 4 illustrates the frequency response plots of the absorber deflection for the optimal control gains and different values of the absorber frequency. It is apparent from these plots that the maximum value of the absorber deflection increases with the increasing value of the absorber frequency. The absorber deflection increases significantly in the low frequency range with the increasing value of the absorber frequency. Thus, (along with the stability requirement) the permissible absorber (actuator) deflection also limits the maximum value of the absorber frequency that can be used in practice.

2.3. Design optimization for improved transient response

It may be noted that the H_∞ optimization discussed in the previous section is suitable for the optimal shaping of the displacement FRF of the primary mass. In this section, the optimization objective is to have a good transient response characteristic featuring low peak response and fast attenuation. For achieving good transient response, the poles of the system should be placed in the left half s-plane at a maximum possible distance from the imaginary axis (for faster attenuation) and minimum possible distance from the real axis (minimum oscillation cycle). Ideally the optimal condition corresponds to equal real parts and zero imaginary parts of the four poles (see Appendix B for proof). However, this makes the poles real and equal, hence critically damped. To be slightly more flexible, one can keep the poles complex (hence underdamped) and the two feedback gains are adjusted such that the damping ratio and the natural frequency of each mode of vibration are optimized for the chosen values of the mass ratio and the absorber frequency. The influences of the absorber frequency and the zeros of the system on the transient response are studied subsequently.

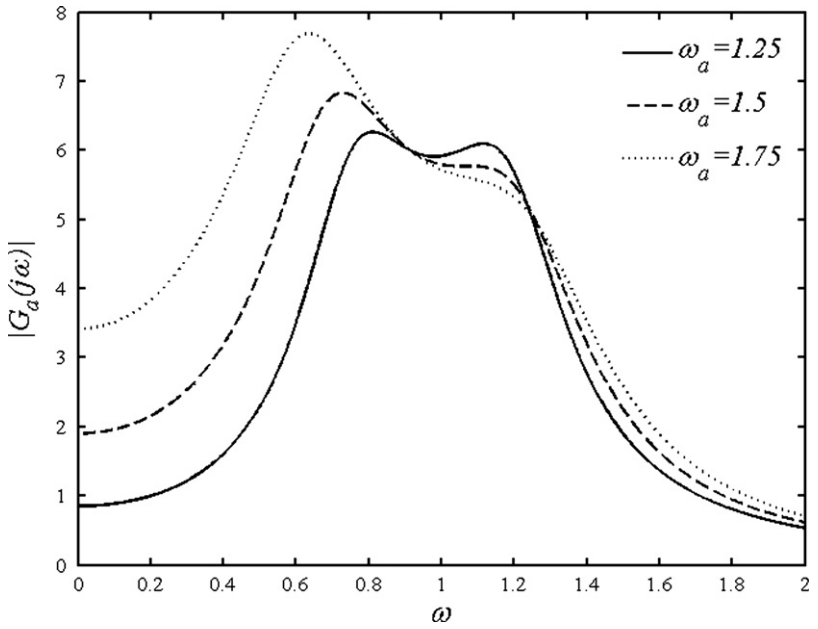

Fig. 4. Frequency response plots of the absorber deflection: μ=0.2.

For complex poles, the design objective is fulfilled by making the two pairs of the complex conjugate eigenvalues of the characteristic equation (Eq. (8)) identical. The proof is as follows.The characteristic equation (Eq.(8)) is expressed in the following form:

$$(s^2+2\xi_1\omega_{n1}s+\omega_{n1}^2)(s^2+2\xi_2\omega_{n2}s+\omega_{n2}^2)=0, \tag{27}$$

where ξ_1 and ξ_2 are the damping ratios and ω_{n1} and ω_{n2} are the natural frequencies of the two modes.Comparing Eqs. (27) and (8) one obtains

$$2r_1+2r_2=a_3, \tag{28}$$

$$4r_1r_2+\omega_{n1}^2+\omega_{n2}^2=a_2, \tag{29}$$

$$2r_1\omega_{n2}^2+2r_2\omega_{n1}^2=a_1=a_3, \tag{30}$$

$$\omega_{n1}^2\omega_{n2}^2=a_0, \tag{31}$$

where $-r_1$ and $-r_2$ are the real parts of the complex poles and are expressed as $r_i=\xi_i\omega_{ni}>0$, i=1, 2.

Eqs. (28) and (30) can be combined to yield

$$2r_1(\omega_{n2}^2-1)+2r_2(\omega_{n1}^2-1)=0. \tag{32}$$

For any desired values of the real parts of the poles, Eq. (32) is satisfied by one natural frequency higher than unity and the other less than unity. However, as a higher value of natural frequency ensures faster response the optimal choice is $\omega_{n1}=\omega_{n2}=1$, for which Eq. (32) is identically satisfied. Under these circumstances, Eq. (31) yields the optimal value of k_p as

$$(k_p)_{opt}=\mu(\omega_a^2-1), \tag{33}$$

when Eqs. (28) and (29) give

$$r_{1,2}=\frac{k_v\pm\sqrt{k_v^2-4\mu^3\omega_a^2}}{4\mu}. \tag{34}$$

Clearly for the chosen values of the mass ratio and the absorber frequency satisfying $k_v^2\geq 4\mu^3\omega_a^2$, r_1 increases and r_2 decreases with the increasing value of k_v. Therefore, the optimal transient response is obtained for $r_1=r_2$ corresponding to the following optimal value of k_v:

$$(k_v)_{opt}=2\omega_a\mu^{3/2}. \tag{35}$$

Thus, the statement that the optimal transient response of the system corresponds to two identical pairs of complex conjugate poles is correct.

The optimal damping (equal for both modes) of the combined system can be obtained as

$$\xi_{\text{opt}} = r_1 = r_2 = \frac{(k_v)_{\text{opt}}}{4\mu} = \frac{1}{2}\omega_a\sqrt{\mu}. \tag{36}$$

It is apparent from Eq. (36) that the optimal damping of the system increases with the increasing frequency of the absorber. Thus, the optimal transient response is achieved through the mode equalization followed by the maximization of the damping. However, as the optimal damping should be less than or equal to unity (as required by the complex pole assumption), the theoretical value of the upper threshold of the absorber frequency should be $2/\sqrt{\mu}$. Clearly, with this value of the absorber frequency, both modes of the system are critically damped.

For any value of the absorber frequency higher than $2/\sqrt{\mu}$, the two complex conjugate pairs of poles transform to two pairs of identical real poles, with one equal pair moving away from the imaginary axis and the other equal pair migrating towards the imaginary axis (this can be proved following the similar analysis as done for the complex poles). Obviously the system becomes overdamped for higher values of the absorber frequency $\omega_a > 2/\sqrt{\mu}$. At this point, it is pertinent to look into the characteristics of the zeros of the system as discussed below.

It is noteworthy that for the optimum gain values, the zeros of the transfer function $G(s)$ given in Eq. (6) are located at $z_{1,2} = -\omega_a\sqrt{\mu} \pm \sqrt{\omega_a^2\mu - 1}$. Clearly, for $\omega_a < 1/\sqrt{\mu}$, the zeros are complex and shift away from the imaginary axis with the increasing value of the absorber frequency thereby rendering the effect of the zeros on the transient response less important. However, beyond $\omega_a > 1/\sqrt{\mu}$ the zeros become real and one of the zeros starts moving towards the imaginary axis and at very high absorber frequency tend to compensate for the adverse effect of the real pole moving towards the imaginary axis. As a whole, the transient response progressively improves with the increasing absorber frequency. The variations of the poles and zeros of the system with the absorber frequency are numerically illustrated in Table 1.

Fig. 5(a) and (b) illustrate the transient response plots of the primary system and the absorber deflection, respectively, with the active absorber optimized according to Eqs. (33) and (35). The transient responses are obtained by direct numerical simulations of equations of motion (Eqs. (4) and (5)). All simulations are run from the initial conditions (1,0,0,0). It is evident from Fig. 5(a) that the transient response of the primary system can be improved by increasing the absorber frequency. However, the maximum absorber deflection increases with the increasing value of the absorber frequency as evident from Fig. 5(b). Therefore, the maximum value of the absorber frequency is limited by the allowable absorber deflection.

Although the absorber optimized according to Eqs. (33) and (35) should ideally be used for improving the transient response of the system, it is also interesting to look into the frequency response characteristics of the system with the absorber optimized for the improved transient response. Such plots are illustrated in Fig. 6(a) and (b). It may be observed from Fig. 6(a) that for a given value of the mass ratio and the absorber frequency, the H_∞ optimal absorber produces relatively reduced amplitude response of the primary mass around the resonance frequency as compared to the absorber

Table 1
Variations of the poles and zeros with the absorber frequency (μ=0.1).

k (ω_a=$k\mu^{-0.5}$)	$(k_p)_{\text{opt}}$	$(k_v)_{\text{opt}}$	Poles of $G(s)$	Zeros of $G(s)$
0.5	0.15	0.1	−0.2500+0.9682i −0.2500−0.9682i −0.2500+0.9682i −0.2500−0.9682i	−0.5000+0.8660i −0.5000−0.8660i
1	0.9	0.2	−0.5000+0.8660i −0.5000−0.8660i −0.5000+0.8660i −0.5000−0.8660i	−1 −1
1.1	1.11	0.22	−0.5500+0.8352i −0.5500−0.8352i −0.5500+0.8352i −0.5500−0.8352i	−0.6417 −1.5583
1.5	2.15	0.3	−0.7500+0.6614i −0.7500−0.6614i −0.7500+0.6614i −0.7500−0.6614i	−0.3820 −2.6180
2	3.9	0.4	−1 −1 −1 −1	−0.2679 −3.7321
5	24.9	1.0	−4.7913 −4.7913 −0.2087 −0.2087	−0.1010 −9.8990

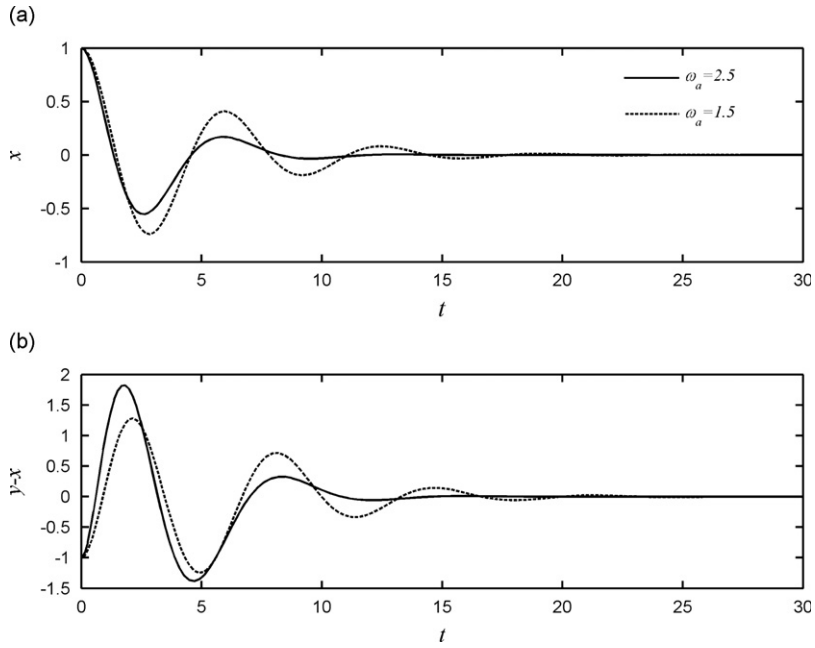

Fig. 5. Numerically simulated transient response plots with the active absorber designed for the improved transient response (maximum damping design): μ=0.2.

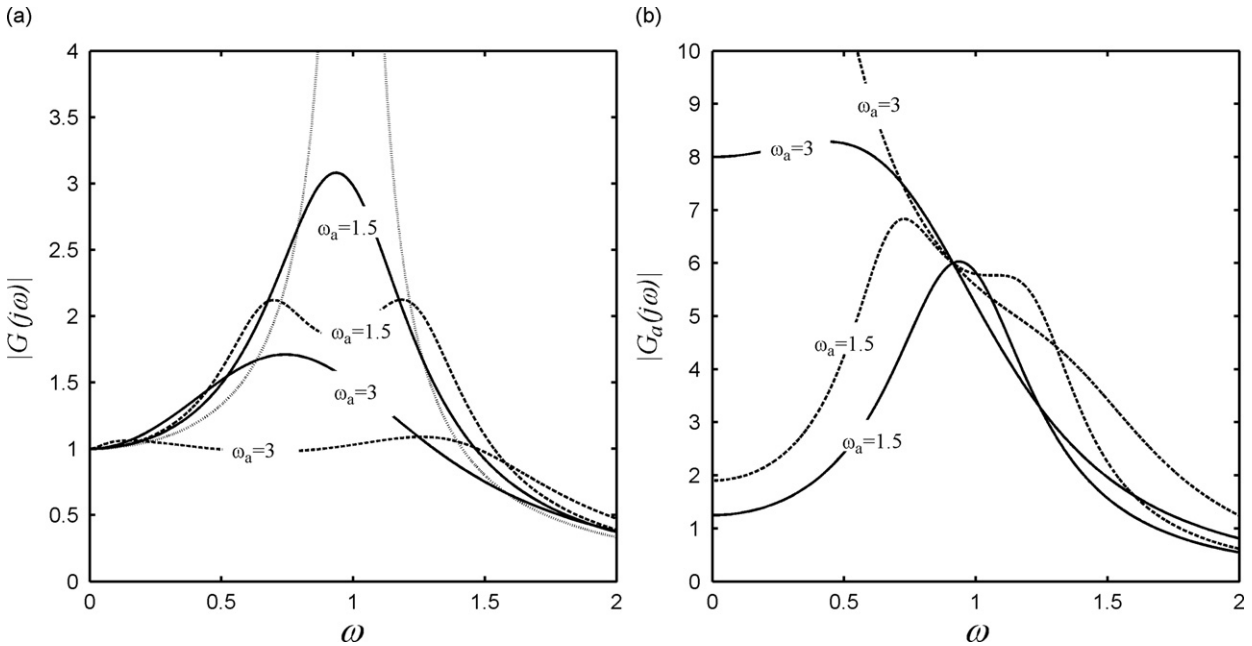

Fig. 6. Comparing frequency response plots of the system with H_∞-optimum active absorber and improved transient response (maximum damping design): (a) displacement of the primary mass; (b) absorber deformation: μ=0.2. ——, maximum damping; - - -, H_∞-optimum; …., without absorber.

optimized for the transient response. However, the deformation characteristics of the absorber optimized for the transient response is relatively better than that of the H_∞ optimal absorber as illustrated in Fig. 6(b).

2.4. Passive absorber vs. the proposed active absorber

A comparative analysis between the optimal performances of the passive DVA and that of the proposed active absorber is presented in this section. The mathematical model of the system with the passive DVA is obtained by substituting the

following expression of the control force in Eq. (4):

$$f_c = c(\dot{x}-\dot{y}), \tag{37}$$

where c is the non-dimensional viscous damping coefficient of the DVA.

The transfer function of the system with the passive absorber relating the displacement of the primary mass and the exciting force is given by

$$G_P(s) = \frac{X(s)}{F(s)} = \frac{s^2+(c/\mu s)+\omega_a^2}{s^4+c_3s^3+c_2s^2+c_1s+c_0}, \tag{38}$$

where $c_3=c+c/\mu$, $c_2 = 1+\omega_a^2+\mu\omega_a^2$, $c_1=c/\mu$, and $c_0 = \omega_a^2$.

2.4.1. Comparing H_∞ optimal performances

The exact solutions of the optimum values (optimum H_∞ norm) of the damping and the frequency of the passive absorber are obtained in Ref. [17] and are given below

$$(\omega_a)_{\text{opt}} = \frac{2}{1+\mu}\sqrt{\frac{32+46\mu+18\mu^2+4(2+\mu)\sqrt{4+3\mu}}{192+240\mu+81\mu^2}}, \tag{39}$$

$$c_{\text{opt}} = \frac{1}{2}\mu(\omega_a)_{\text{opt}}\sqrt{\frac{8+9\mu-4\sqrt{4+3\mu}}{1+\mu}}. \tag{40}$$

An approximate expression of the optimized peak frequency response is obtained as

$$|G_P(\mathrm{j}\omega)|_{\max} \approx \sqrt{\frac{2+\mu}{\mu}}. \tag{41}$$

It is already mentioned that, unlike the passive absorber, the active absorber does not require having its frequency close to the natural frequency of the primary system and a higher value of the frequency of the active absorber is always beneficial. From Eqs. (41) and (25) one obtains the ratio (R) of the peak value of the displacement frequency response of the primary system with the active tp that with the passive absorber as

$$R = \frac{|G(\mathrm{j}\omega)|_{\max}}{|G_P(\mathrm{j}\omega)|_{\max}} = \frac{1}{\omega_a}\sqrt{\frac{2}{2+\mu}}. \tag{42}$$

From Eq. (42) it is apparent that R is less than unity if the frequency of the active absorber $\omega_a > \sqrt{2/2+\mu}$. Indeed, a higher value of the frequency of the active absorber yields a smaller value of R entailing a better performance of the active absorber as compared to the passive one. Fig. 7(a) compares the displacement frequency response plots of the primary mass with the passive and the active absorber both optimized (H_∞ optimization) for the mass ratio μ=0.2. Clearly, the active absorber produces a better frequency response characteristic over a wider frequency band around the resonance frequency of the primary system. It is observed from Fig. 7(b) and (c) that with the increasing values of the absorber frequency and the mass ratio, the performance of the active absorber turns progressively superior to that of the passive absorber in terms of both the suppression bandwidth as well as the FRF, particularly around the resonance frequency of the primary system.

2.4.2. Comparing performances for optimal transient response

Following the similar procedure as discussed in Section 2.3, one obtains the expressions of the optimum absorber frequency and damping corresponding to the optimal transient response of the combined system with the passive absorber as

$$(\omega_a)_{\text{opt}} = \frac{1}{1+\mu}, \tag{43}$$

and

$$c_{\text{opt}} = 2\left(\frac{\mu}{1+\mu}\right)^{3/2}. \tag{44}$$

The corresponding optimum damping of the combined system with the passive absorber becomes

$$\xi_{\text{opt}} = \frac{1}{2}\sqrt{\mu}. \tag{45}$$

From Eq. (45) it is known that the optimal damping of the system with the passive absorber can be increased only by increasing the mass ratio. However, as the maximum value of mass ratio that can be used in practice is usually small, the maximum achievable damping is also limited. However, Eq. (36) suggests that for a given value of the mass ratio, the

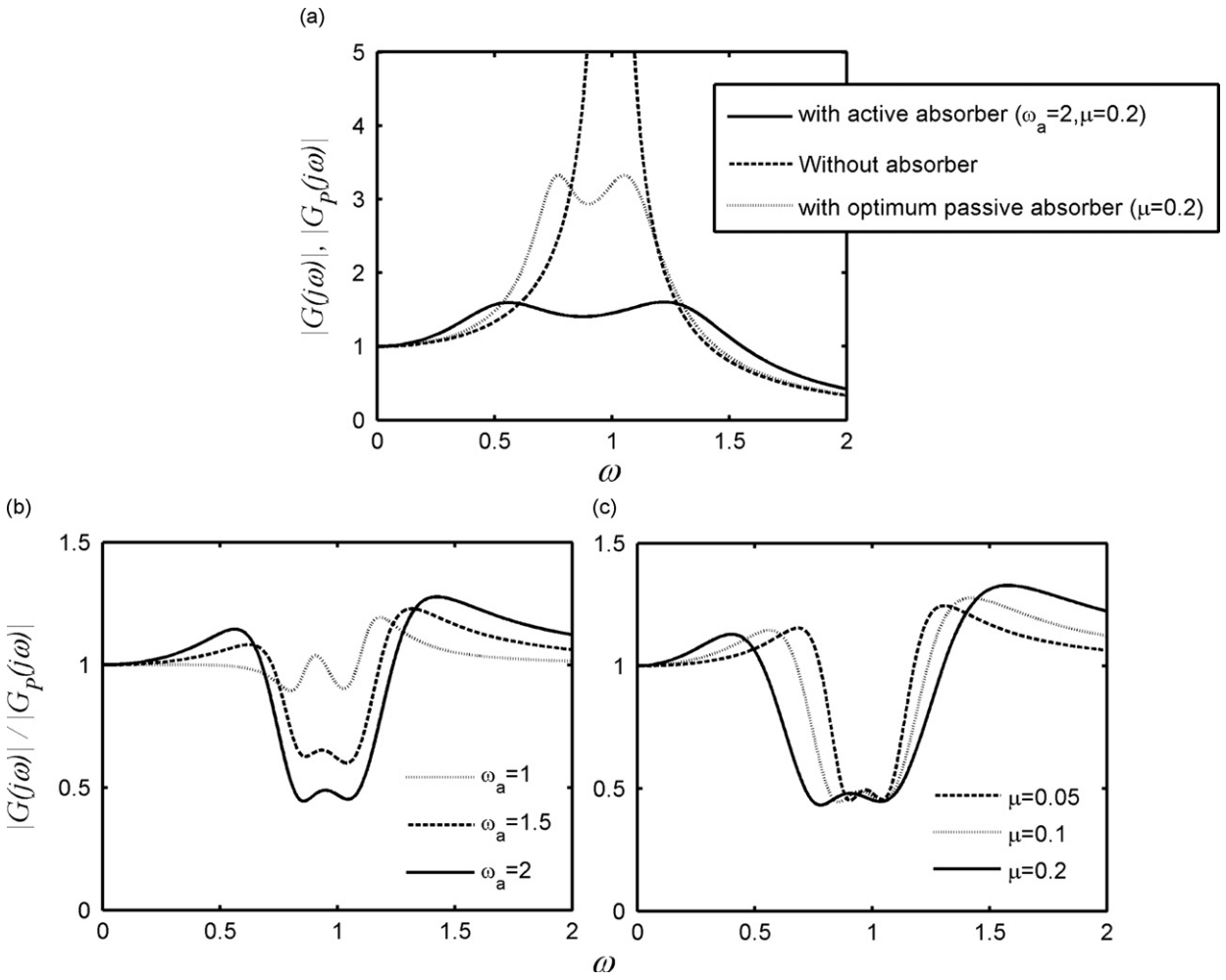

Fig. 7. Comparisons of the frequency responses of the system with the H_∞-optimum active and passive absorbers: (a) μ=0.2, (b) μ=0.1, and (c) ω_a=2.0. Passive absorber is optimized according to Eqs. (37) and (38). Active absorber is optimized according to Eqs. (15) and (22).

optimal damping of the system with the active absorber can be increased by increasing the absorber frequency. Comparing Eq. (36) with Eq. (45) it is evident that for a given value of the mass ratio, the optimal damping produced by the active absorber is higher than that produced by the passive absorber if the frequency of the active absorber is selected greater than unity. Thus, a better transient response as well as the frequency response can be achieved with the proposed active absorber.

The transient responses of the primary system with the passive and the active absorber both designed for the optimal transient response are compared in Fig. 8. It is observed from Fig. 8 that the transient response performance of the system with the optimized active absorber is better than that with the optimum passive absorber. Fig. 9 confirms that the active absorber designed for optimum transient response can produce better frequency response characteristics compared to that is achievable with the optimized (any of the two forms of the optimization discussed) passive absorber.

3. Elastic beam as the primary system

3.1. Mathematical model

In this section, the primary system is considered as a general Euler–Bernoulli beam. The beam is excited by a point force F_e at the location b and the absorber is attached at the location a as illustrated in Fig. 10. The geometric and physical properties of the beam are assumed to be uniform along the length. The elastic deformation of the beam about the neutral axis is denoted by $X(t, Z)$, where t is the time variable and Z is the position variable along the beam.

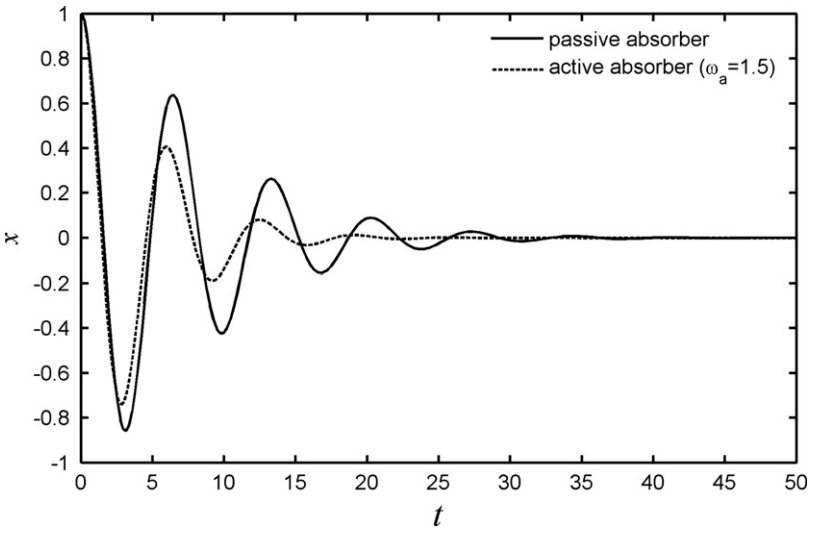

Fig. 8. Comparison of the simulated transient response of the system with the active and passive absorbers both designed for improved transient response (maximum damping design): μ=0.2. Initial conditions are (1,0,0,0).

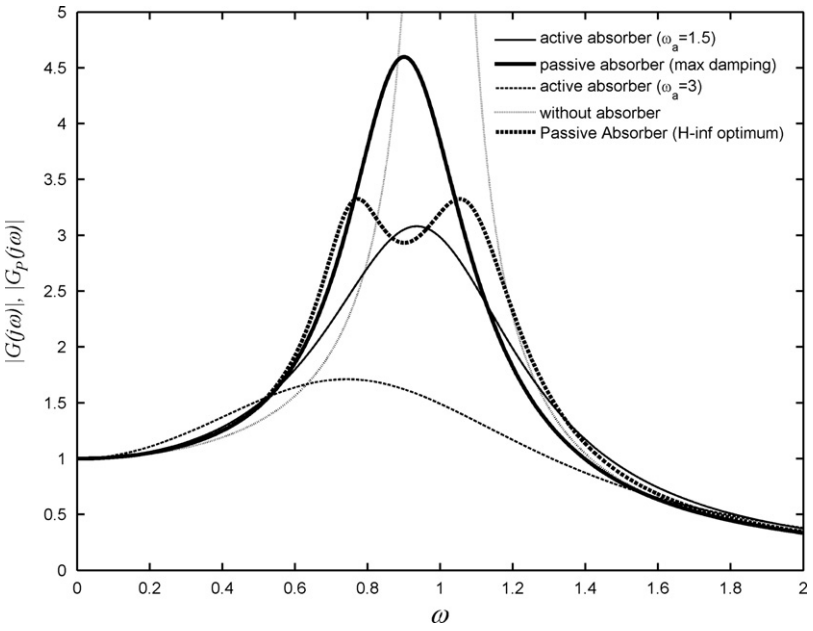

Fig. 9. Comparisons of the frequency response plots of the system with the active absorber designed for improved transient response (maximum damping design) and the optimum passive absorber: μ=0.2.

Using the *Galerkin approximation* [20], the beam deflection can be represented by a finite sum (up to n modes) as

$$X(t^*,Z) = \sum_{i=1}^{n} \phi_i(Z) q_i(t), \tag{46}$$

where $\phi_i(Z)$ is the mode shape function and $q_i(t)$ is the modal displacement of the ith mode of the beam vibration.

The control force is the linear combination of the states of the absorber mass as expressed below

$$F_c = -(K_p q_a - K_v \dot{q}_a), \tag{47}$$

where K_v and K_p are the control gains and q_a is the displacement of the absorber mass. The dot $(\cdot)$ denotes the derivative with respect to the time variable t.

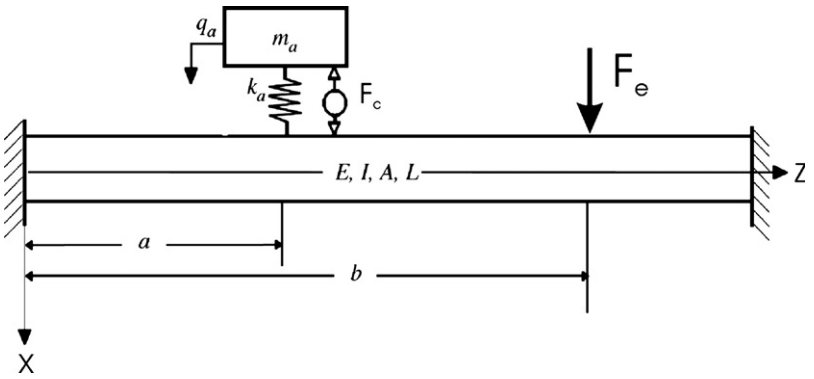

Fig. 10. Beam with the attached active absorber.

The dynamics of the beam-absorber system is governed by the following differential equations:

$$M_i\ddot{q}_i(t)+K_iq_i(t)+k_a\left\{\sum_{i=1}^{n}\phi_i(a)q_i(t)-q_a(t)\right\}\phi_i(a)=-\phi_i(a)\{K_Pq_a(t)-K_v\dot{q}_a(t)\}+\phi_i(b)F_e(t),\quad i=1,2,\ldots,n, \tag{48}$$

$$m_a\ddot{q}_a(t)-k_a\left\{\sum_{i=1}^{n}\phi_i(a)q_i(t)-q_a(t)\right\}=K_Pq_a(t)-K_v\dot{q}_a(t). \tag{49}$$

M_i and K_i are defined as

$$M_i=\rho A\int_0^L\phi_i^2(Z)\,dZ, \tag{50}$$

and

$$K_i=EI\int_0^L\left\{\frac{\partial^2}{\partial Z^2}(\phi_i(Z))\right\}^2dZ, \tag{51}$$

where ρ is the density, E is the elastic modulus, I is the area moment of inertia, A is the cross-sectional area, and L is the length of the beam.

Considering the normalization criterion as $\int_0^L\phi_i^2(Z)\,dZ=L$, one can rewrite Eqs. (48) and (49) in the following non-dimensional forms:

$$\ddot{x}_i(\tau)+\omega_{ni}^2x_i(\tau)+\mu\omega_a^2\left\{\sum_{i=1}^{n}\phi_i(a)x_i(\tau)-y(\tau)\right\}\phi_i(a)+\phi_i(a)\{k_py(\tau)-k_v\dot{y}(\tau)\}=\phi_i(b)f(\tau),\quad i=1,2,\ldots,n \tag{52}$$

$$\mu\ddot{y}(\tau)+k_v\dot{y}(\tau)+(\mu\omega_a^2-k_p)y(\tau)=\mu\omega_a^2\sum_{i=1}^{n}\phi_i(a)x_i(\tau). \tag{53}$$

The non-dimensional quantities in Eqs. (52) and (53) are as defined below

$$\text{Non-dimensional } i\text{th Modal displacement of the beam}: x_i=\frac{q_i}{\delta_{st}},$$

where δ_{st} is the static deflection of the beam under unit load at the location of the point force.

$$\text{Non-dimensional absorber displacement}: y=\frac{q_a}{\delta_{st}}.$$

$$\text{Mass ratio}: \mu=\frac{m_a}{m_b}\ \text{ where the mass of the beam } m_b=\rho AL.$$

$$\text{Non-dimensional natural frequency of the absorber}: \omega_a=\frac{1}{\omega_0}\sqrt{\frac{k_a}{m_a}},$$

where ω_0 is the reference frequency, which may be conveniently taken as the first natural frequency of the beam.ω_{ni} is the ith natural frequency of the beam normalized by the reference frequency ω_0.

$$\text{The non-dimensional excitation force}: f=\frac{F_e}{m_b\omega_0^2\delta_{st}}.$$

The non-dimensional control gains are $k_p = \dfrac{K_p}{m_b\omega_0^2}$ and $k_v = \dfrac{K_v}{m_b\omega_0}$.

The dot $(\cdot)$ in Eqs. (52) and (53) denotes differentiation with respect to the non-dimensional time $\tau=\omega_0 t$.

3.2. Stability and frequency response characteristics of the combined system

In the Laplace domain, Eqs. (52) and (53) can be written as

$$[\mathbf{P}(\mathbf{s})]\{\mathbf{U}(\mathbf{s})\} = \{\mathbf{\Phi}(\mathbf{b})\}F(s), \tag{54}$$

where $\{\mathbf{U}(\mathbf{s})\} = \{\, X_1(s) \quad X_2(s) \quad . \quad . \quad . \quad X_n(s) \quad Y(s) \,\}^{\mathrm{T}}$, $\{\mathbf{\Phi}(\mathbf{b})\} = \left\{\, \phi_1(b) \quad \phi_2(b) \quad . \quad . \quad . \quad \phi_n(b) \quad 0 \,\right\}^{\mathrm{T}}$, and

$$[\mathbf{P}(\mathbf{s})] = \begin{bmatrix} s^2+\omega_{n1}^2+\mu\omega_a^2\phi_1^2(a) & \mu\omega_a^2\phi_1(a)\phi_2(a) & . \; . & \mu\omega_a^2\phi_1(a)\phi_n(a) & \alpha_1(s) \\ \mu\omega_a^2\phi_2(a)\phi_1(a) & s^2+\omega_{n2}^2+\mu\omega_a^2\phi_2^2(a) & . \; . & \mu\omega_a^2\phi_2(a)\phi_n(a) & \alpha_2(s) \\ . & . & . \; . & . & . \\ . & . & . \; . & . & . \\ \mu\omega_a^2\phi_n(a)\phi_1(a) & \mu\omega_a^2\phi_n(a)\phi_2(a) & . \; . & s^2+\omega_{nn}^2+\mu\omega_a^2\phi_n^2(a) & \alpha_n(s) \\ \beta_1 & \beta_2 & . \; . & \beta_n & \mu s^2+k_v s+\lambda \end{bmatrix} \tag{55}$$

with $\alpha_i(s) = -\phi_i(a)\{\lambda+k_v s\}$, $i=1, 2, 3, \ldots, n$, $\beta_i = -\mu\omega_a^2\phi_i(a)$ and $\lambda = \mu\omega_a^2 - k_p$.

The stability of the system is determined by the characteristic equation given by

$$\det([\mathbf{P}(\mathbf{s})]) = 0. \tag{56}$$

Using the Routh–Hurwitz criterion one can show after lengthy algebraic manipulations that the combined system is stable if conditions given in Eq. (10) are satisfied, i.e., both k_v and λ are positive.

The transfer function relating the beam deflection at the point of attachment of the absorber and the exciting force can be obtained as

$$G(s) = \sum_{i=1}^{n} \phi_i(a) G_i(s), \tag{57}$$

where the ith modal transfer function $G_i(s)$ is defined as the ith row of the matrix $[\mathbf{P}(\mathbf{s})]^{-1}\{\mathbf{\Phi}(\mathbf{b})\}$.

3.2.1. Quasi-optimal absorber

Unlike the single-degree-of-freedom case, the MDOF system does not seem to have a closed form solution for the optimum parameter values of the absorber. However for the primary systems having widely separated modal frequencies, one can still use the methods developed in Section 2 for obtaining the quasi-optimal values of the absorber parameters (k_p and k_v) for a single mode if the effects of the other modes are neglected. Neglecting the effects of the other modes, the dynamics of the combined system considering only the ith mode of the primary system are obtained from Eqs. (52) and (53) as

$$\ddot{x}_i(\tau) + \omega_{ni}^2 x_i(\tau) + \mu\omega_a^2\phi_i^2(a)x_i(\tau) + \phi_i(a)\{k_p y(\tau) - k_v\dot{y}(\tau)\} = \phi_i(b) f(\tau), \tag{58}$$

$$\mu\ddot{y}(\tau) + k_v\dot{y}(\tau) + (\mu\omega_a^2 - k_p)y(\tau) = \mu\omega_a^2\phi_i(a)x_i(\tau). \tag{59}$$

Now following the similar procedure as described in Section 2.2.1, one obtains the following expression for H_∞ optimal value of the parameter k_p:

$$(k_p)_{\mathrm{opt}} = \mu\left\{\left(\frac{\mu\phi_i^2(a)}{2}+1\right)\omega_a^2 - \omega_{ni}^2\right\}. \tag{60}$$

The corresponding optimal expression of the parameter k_v is obtained according to Eq. (24), where $(k_v)_1$ and $(k_v)_2$ are obtained as the positive solutions of Eqs. (61) and (62), respectively

$$\tilde{g}_4 k_v^4 + \tilde{g}_2 k_v^2 + \tilde{g}_0 = 0, \tag{61}$$

where

$$\tilde{g}_4 = \omega_{ni}^2\left\{4\omega_{ni}\omega_a\phi_i(a)\mu - \sqrt{2}\omega_a^2\phi_i^2(a)\mu^{3/2} - 2\sqrt{2}\omega_{ni}^2\sqrt{\mu}\right\},$$

$$\tilde{g}_2 = \omega_{ni}\omega_a^2\phi_i^2(a)\mu^3\left\{-2\omega_{ni}^2\omega_a\phi_i(a)\mu + 2\sqrt{2}\omega_{ni}^3\sqrt{\mu} + \omega_a^3\phi_i^3(a)\mu^2 - \sqrt{2}\omega_{ni}\omega_a^2\phi_i^2(a)\mu^{3/2}\right\}$$

and

$$\tilde{g}_0 = -\frac{1}{8}\omega_a^4\phi_i^4(a)\mu^6\left\{32\omega_{ni}^3\omega_a\phi_i(a)\mu - 12\sqrt{2}\omega_{ni}^2\omega_a^2\phi_i^2(a)\mu^{3/2} - 12\sqrt{2}\omega_{ni}^4\mu^{1/2} + \sqrt{2}\omega_a^4\phi_i^4(a)\mu^{5/2}\right\}$$

$$\tilde{h}_4 k_v^4 + \tilde{h}_2 k_v^2 + \tilde{h}_0 = 0, \tag{62}$$

where

$$\tilde{h}_4 = \omega_{ni}^2\left\{4\omega_{ni}\omega_a\phi_i(a)\mu + \sqrt{2}\omega_a^2\phi_i^2(a)\mu^{3/2} + 2\sqrt{2}\omega_{ni}^2\sqrt{\mu}\right\},$$

$$\tilde{h}_2 = \omega_{ni}\omega_a^2\phi_i^2(a)\mu^3\left\{-2\omega_{ni}^2\omega_a\phi_i(a)\mu - 2\sqrt{2}\omega_{ni}^3\sqrt{\mu} + \omega_a^3\phi_i^3(a)\mu^2 + \sqrt{2}\omega_{ni}\omega_a^2\phi_i^2(a)\mu^{3/2}\right\}$$

and

$$\tilde{h}_0 = -\frac{1}{8}\omega_a^4\phi_i^4(a)\mu^6\left\{32\omega_{ni}^3\omega_a\phi_i(a)\mu + 12\sqrt{2}\omega_{ni}^2\omega_a^2\phi_i^2(a)\mu^{3/2} + 12\sqrt{2}\omega_{ni}^4\mu^{1/2} - \sqrt{2}\omega_a^4\phi_i^4(a)\mu^{5/2}\right\}.$$

In order to maintain the stability of the combined system, the absorber frequency must satisfy the following relationship:

$$\omega_a < \frac{\omega_{ni}}{\phi_i(a)}\sqrt{\frac{2}{\mu}}. \tag{63}$$

Following the similar procedure as described in Section 2.2.1, the optimal parameter values for the transient response of a particular mode can be obtained as

$$(k_p)_{\text{opt}} = \mu(\omega_a^2 - \omega_{ni}^2), \tag{64}$$

and

$$(k_v)_{\text{opt}} = 2\phi_i(a)\omega_a\mu^{3/2}. \tag{65}$$

3.2.2. Numerical example

As numerical examples, the displacement frequency response functions of a simply supported beam with the proposed absorber attached to it are evaluated. The first three modes of the beam are used to evaluate the frequency response functions according to Eq. (57). The first three non-dimensional modal frequencies of the beam are 1, 4 and 9. First, the optimizations are performed with the objective of controlling the vibration of the first mode and the corresponding frequency response plots are illustrated in Fig. 11. The frequency response plots with the absorber optimized to control the second mode are shown in Fig. 12. It is observed from these frequency response plots that the optimal absorber can control the targeted mode to a greater extent. In the example FRF plots in Figs. 11 and 12, the modes other than the targeted mode are also observed to be controlled

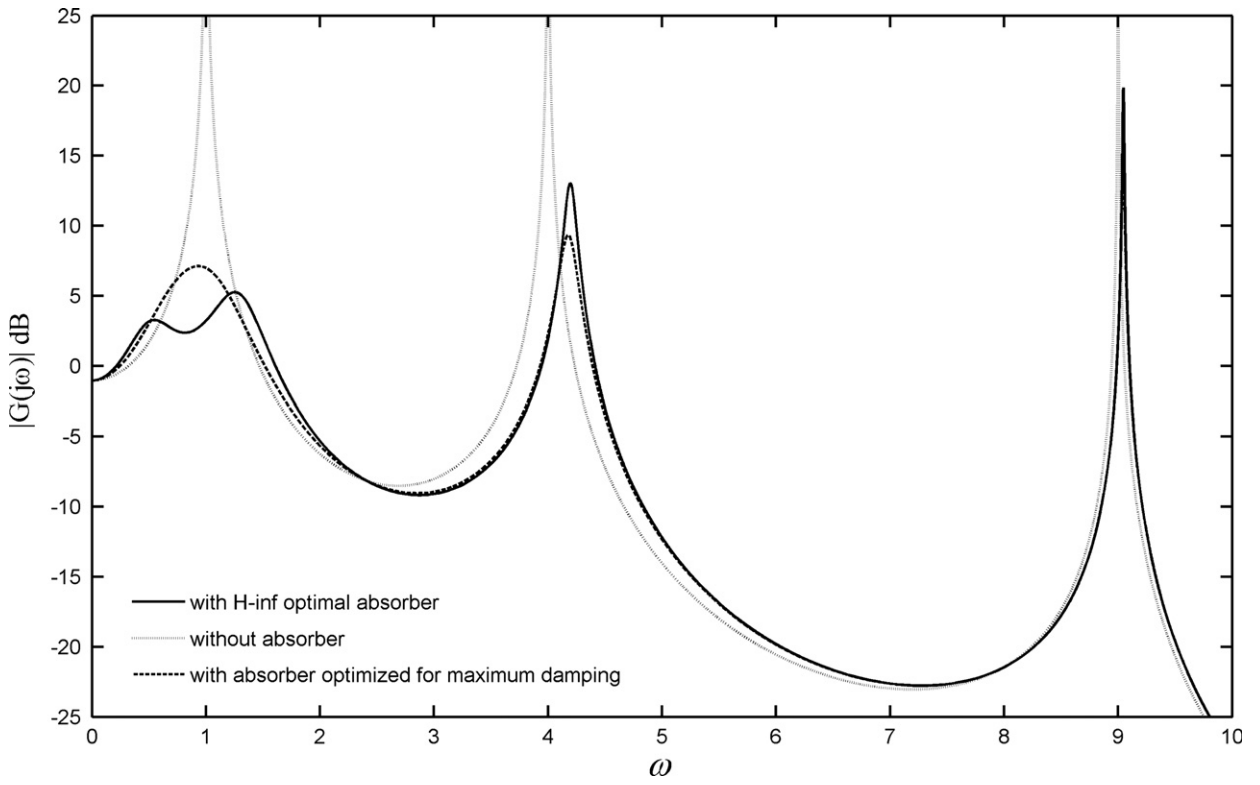

Fig. 11. Frequency response plot of the beam deflection at the location of the absorber: ω_a=2, μ=0.2, a=0.25, b=0.75. The optimum design is centered on the first mode.

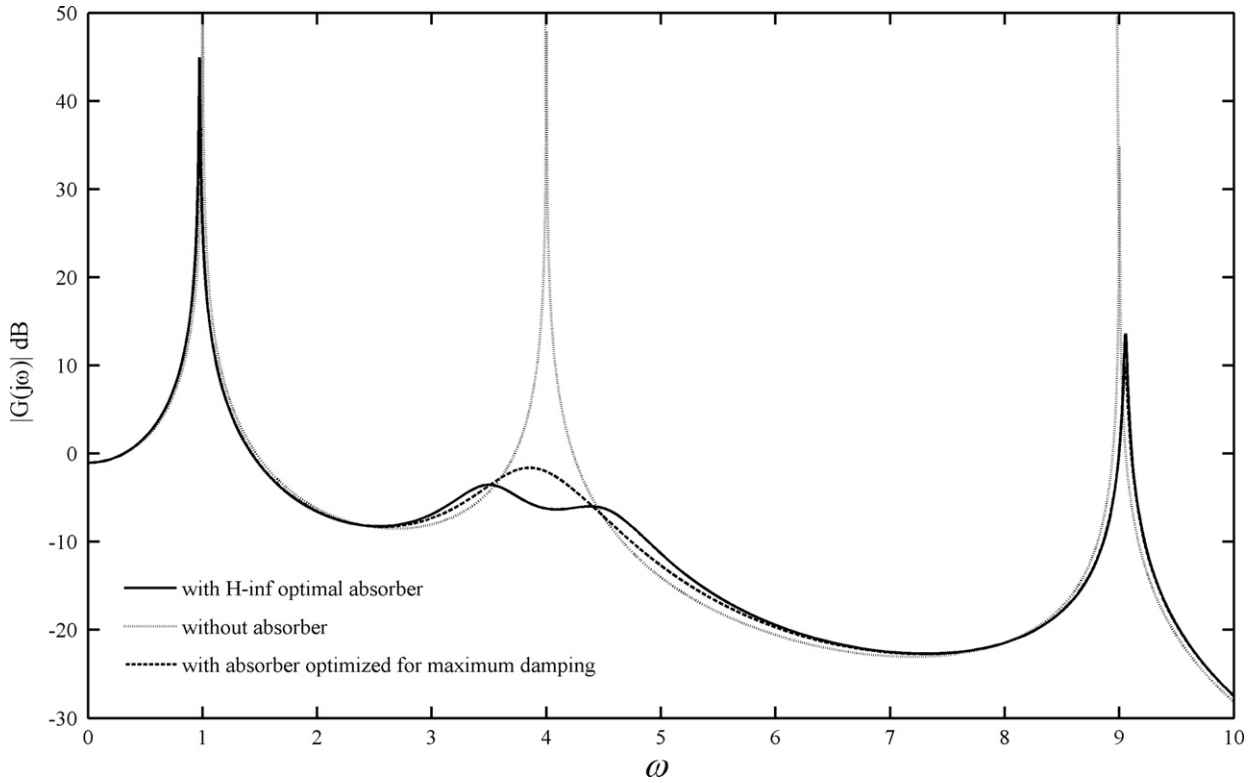

Fig. 12. Frequency response plot of the beam deflection at the location of the absorber: ω_a=2, μ=0.2, a=0.25, b=0.75. The optimum design is centered on the second mode.

though to somewhat lesser extent. However, there is no solid theoretical evidence that the non-targeted modes are actually controlled. If required, multiple absorbers can be used in practice to exercise separate control actions on individual modes.

4. Conclusions

The present study investigates the efficacy of an active vibration absorber in controlling resonant and transient vibrations of linear vibratory systems. The absorber consists of a spring–mass system with an actuator operating parallel to the spring. The actuator is controlled by the state feedback taken from the absorber mass. As the absorber runs on the state feedback of the absorber mass, it is self-contained and does not require any sensory inputs from outside. This standalone feature makes it user-friendly as well as commercially very attractive. The proposed active absorber with the optimal parameter tuning has shown to have performed better than a passive absorber.

Initially, the primary structure is considered to be a single-degree-of-freedom system and the conditions of the stability of the combined system are derived. Employing the formal fixed-point theory, expressions for the optimal parameter values of the absorber are determined. The following two types of optimization criteria are used:

1. H_∞ optimization for the optimal shaping of the frequency response function.
2. Optimization for improved transient response.

The frequency and the transient responses of the system with the optimized active and passive absorbers are compared. The major comparative differences are listed below

(i) Unlike the passive absorber, the frequency for the active absorber should not have to be equal to the natural frequency of the primary system. In fact, the absorber frequency can assume any value without violating the stability limit and the permissible actuator deflection.

(ii) The suppression bandwidth around the resonance frequency of the primary system increases and the frequency response within the suppression bandwidth decreases with the increasing value of the absorber frequency. For the H_∞ optimal absorber, there is an upper threshold value of the absorber frequency determined by the stability requirement. For a given mass ratio, the optimal active absorber can produce a much better frequency response than that is achieved using an optimal passive absorber.

(iii) The absorber optimized for the improved transient response can theoretically attain any value of the damping depending upon the absorber frequency and the mass ratio. The damping of the system increases linearly with the

absorber frequency. As a result, the optimal active absorber produces a better transient response than that achieved by the optimal passive absorber.

The efficacy of the active absorber in controlling the forced vibration of an Euler–Bernoulli beam is also analyzed. For the beam like primary structure, the optimization of the absorber parameters is carried out on the modal basis following the similar procedure employed in case of the single-degree-of-freedom primary system. It is shown that the optimal absorber can exercise a good degree of control on the targeted mode.

Appendix A

In this section, it is proved that the frequency response function of the primary system attached with the proposed active absorber passes though two fixed points irrespective of the gain parameter k_v. Substituting $s=\mathrm{j}\omega$ in the expression of the transfer function of the system given in Eq. (6), the frequency response function of the primary system is expressed in the following form:

$$|G(\mathrm{j}\omega)| = \sqrt{\frac{A^2+k_v^2B^2}{C^2+k_v^2D^2}}, \tag{A.1}$$

where

$$A = \mu(a_0-\omega^2),$$

$$B = \omega,$$

$$C = \mu(\omega^4-a_2\omega^2+a_0),$$

$$D = \omega(1-\omega^2).$$

The frequency response function in Eq. (A.1) is independent of k_v if the following condition is satisfied:

$$\frac{A}{C} = \pm\frac{B}{D}, \tag{A.2}$$

which is equivalent to

$$\frac{a_0-\omega^2}{\omega^4-a_2\omega^2+a_0} = \pm\frac{1}{1-\omega^2}. \tag{A.3}$$

The positive sign in the right-hand side expression in Eq. (A.3) yields the trivial solution of the frequency for which the frequency response is independent of k_v. For the negative sign in the right-hand side expression, Eq. (A.3) is rewritten as

$$\omega^4-\frac{1}{2}(a_2+a_0+1)\omega^2+a_0 = 0. \tag{A.4}$$

Clearly if two non-trivial roots of Eq. (A.4) are ω_1^2 and ω_2^2 one writes

$$\omega_1^2+\omega_2^2 = \frac{1}{2}(a_2+a_0+1) > 0. \tag{A.5}$$

Therefore, the roots of Eq. (A.4) are real and positive. Thus, there exists two non-trivial frequencies at which the frequency response function is independent of the parameter value k_v. This proves the fixed-point phenomenon for the proposed system.

Appendix B

For achieving faster attenuation, the real parts of the poles should be placed at the maximum possible distance from the imaginary axis in the left half s-plane. Whereas the maximum overall damping of the system and the minimum number oscillation cycles of the transient response may be achieved by making the imaginary parts of the poles as low as possible.

Denoting the roots of the characteristic equation (Eq. (8)) as λ_i ($i=1, 2, 3, 4$), one writes

$$-\sum_{i=1}^{4}\mathrm{Re}(\lambda_i) = a_3 = \frac{k_v}{\mu}. \tag{B.1}$$

Eq. (B.1) implies that

$$\min_{i=1,\ldots,4}(|\mathrm{Re}(\lambda_i)|) \le \frac{k_v}{4\mu}. \tag{B.2}$$

Eq. (B.2) clearly suggests that the maximization of the absolute values of the real parts of the poles is achieved when the real parts of all the four poles are made equal by tuning the absorber parameters. As the minimum possible value of the

imaginary parts is zero, the optimum performance of the absorber requires that all the four poles are real (negative) and equal.

References

[1] H. Frahm, Devices for damping vibrations of bodies, U.S. Patent #989958, 1911.
[2] J.P. Den Hartog, J. Ormondroyd, Theory of the dynamic vibration absorber, *Transactions of the ASME, Journal of Applied Mechanics* 50-7 (1928) 11–22.
[3] H.-N. Li, X.-L. Ni, Optimization of non-uniformly distributed multiple tuned mass damper, *Journal of Sound and Vibration* 308 (2007) (2007) 80–97.
[4] J.Q. Sun, M.R. Jolly, M.A. Norris, Passive, adaptive, and active tuned vibration absorbers—a survey, *ASME Transactions* 117 (1995) 234–242 (Special 50th Anniversary, Design Issue).
[5] L. Kela, P. Vähäoja, Recent studies of adaptive tuned vibration absorbers/neutralizers, *ASME, Applied Mechanics Review* 62 (2009) 1–9.
[6] J.H. Koo, M. Ahmadian, M. Setareh, T. Murray, In search of suitable control methods for semi-active tuned vibration absorbers, *Journal of Vibration and Control* 10 (2) (2004) 163–174.
[7] N. Olgac, B. Holm-Hansen, A novel active vibration absorption technique: delayed resonator, *Journal of Sound and Vibration* 176 (1994) 93–104.
[8] N. Olgac, M. Hosek, Active vibration absorption using delayed resonator with relative position measurement, *Journal of Vibration and Acoustics* 119 (1997) 131–136.
[9] D. Filipovic, N. Olgac, Torsional delayed resonator with speed feedback, *IEEE/ASME Transactions on Mechatronics* **3** (1) (1998) 67–72.
[10] N. Olgac, H. Elmali, M. Hosek, M. Renzulli, Active vibration control of distributed systems using delayed resonator with acceleration feedback, *Journal of Dynamic Systems, Measurement and Control* 119 (1997) 380–389.
[11] D. Knowles, N. Jalili, S. Ramadurai, Piezoelectric structural vibration control using active resonator absorber, *Proceedings of the 2001 International Mechanical Engineering Congress and Exposition (IMECE'01)*, 2001, New York.
[12] H. Elmali, M. Renzulli, N. Olgac, Experimental comparison of delayed resonator and PD controlled vibration absorbers using electromagnetic actuators, *ASME Journal of Dynamic Systems, Measurement and Control* 122 (2000) 514–520.
[13] N. Jalili, N. Olgac, Optimum delayed feedback vibration absorber for flexible beams, *Smart Structures*, NATO Science Series, Vol. 65, Kluwer Academic, Amsterdam, 1999, pp. 237–246.
[14] N. Jalili, N. Olgac, A sensitivity study on optimum delayed feedback vibration absorber, *ASME Journal of Dynamic Systems, Measurement and Control* 122 (2000) 314–321.
[15] Y. Okada, K. Matsuda, H. Hashitani, Self-sensing active vibration control using the moving-coil-type actuator, *Journal of Vibrations and Acoustics* 117 (1995) 411–415.
[16] H. Rivaz, R. Rohling, An active dynamic vibration absorber for a hand-held vibro-elastography probe, *ASME Journal of Vibration and Acoustics* 129 (2007) 101–112.
[17] S. Huyanan, N.D. Sims, Vibration control strategies for proof-mass actuators, *Journal of Vibration and Control* 13 (12) (2007) 1785–1806.
[18] T. Asami, O. Nishihara, A.M. Baz, Analytical solutions to H_∞ and H_2 optimization of dynamic vibration absorbers attached to damped linear systems, *ASME Journal of Vibration and Acoustics* 124 (2002) 284–295.
[19] J.P. Den Hartog, *Mechanical Vibrations* (1956) 93–104.
[20] C.W. de Silva, *Computer Techniques in Vibration*, CRC Press, 2007.